Mechanics and Mechanical Engineering
Vol. 7, No. 1 (2004) 15–22

Models of the Fracture Harmonic Vibration of the Multi-layered Composites

Mieczyslaw JARONIEK
Division of Strength of Materials and Structures, Technical University of Lodz
Stefanowskiego 1/15, 90-924 Lodz, Poland

Received (19 August 2003)
Revised (4 September 2003)
Accepted (10 November 2003)

Advanced mechanical and structural applications require accurate assessment of the damage state of materials during the fabrications as well as during the service. Due to the complex nature of the internal structure of the material, composites including the layered composite often fail in a variety of modes. The failure modes very often are influenced by the local material properties that may develop in time under heat and pressure, local defect distribution, process induced residual stress, and other factors. Consider a laminate composite in plane stress conditions, multi-layered beam bonded to planes having shear modulus G_i and Poisson's ratio ν_I respectively, subjected to bending. The behaviour of the cracks depends on the cracks configuration, size, orientation, material properties, and loading characteristic. The fracture mechanics problem will be attacked using the photoelastic visualization of the fracture events in a model structure. The proposed experimental method will developed fracture mechanics tools for a layered composite fracture problem.

Keywords: composites, reinforced beams, fracture mechanic, photoelastic method, finite element method.

1. Introduction

The development of the failure criterion for a particular application is also very important for the predictions of the crack path and critical loads.

Recently, there has been a successful attempt to formulate problems of multiple cracks without any limitation. This attempt was concluded with the series of papers summarizing the undertaken research for isotropic [2], an isotropic [4] and non-homogeneous class of problems [5] and [4].

Crack propagation in multi-layered composites of finite thickness is especially challenging and open field for investigation. Some results have been recently reported in [5]. The numerical calculations were carried out using the finite element programs ANSYS 5.4 and 5.6 [11]. Two different methods were used: solid modeling and direct generation.

2. Material properties

Material properties exert an influence on the stress distribution and concentration, damage process and load carrying capacity of elements. In the case of elastic-plastic materials, a region of plastic strains originates in most heavily loaded cross-sections. In order to visualize the state of strains and stresses, some tests have been performed on the samples made of an "araldite"-type optically active epoxy resin (Ep-53), modified with softening agents in such a way that an elastic material has been obtained. Properties of the components of experimental model are given in Table 1.

Table 1 Mechanical properties of the experimental model components

Layer	Young's modulus $\mathbf{E}_i$ [MPa]	Poisson's ratio in terms of stresses $\nu_i[1]$	Photoelastic constants in terms of stresses k_σ [MPa/fr.]	Photoelastic constants in terms of strain $f_\epsilon[-/fr]$
1	3450.0	0.35	1.68	$6.572 \cdot 10^{-4}$
2	1705.0	0.36	1.18	$9.412 \cdot 10^{-4}$
3	821.0	0.38	0.855	$14.31 \cdot 10^{-4}$
4	683.0	0.40	0.819	$16.79 \cdot 10^{-4}$

3. Experimental Results

The stress distribution in was determined using two methods: **Shear Stress Difference Procedure** (SDP – evaluation a complete stress state by means the isochromatics and the angles of the isoclines along the cuts) [3]. **Method of the characteristics** (the stress distribution were determined using the isochromatics only and the equations of equilibrium [10]. In a general case [7], the Cartesian components of stress: σ_x , σ_y and τ_{xy} in the neighbourhood of the crack tip are:

$$\begin{aligned}
\sigma_x &= \frac{1}{\sqrt{2\pi r}} K_I \left[K_i \cos\frac{\Theta}{2}\left(1 - \sin\frac{\Theta}{2}\sin\frac{3\Theta}{2}\right) \right. \\
&\quad \left. -K_{II}\sin\frac{\Theta}{2}\left(2 + \cos\frac{\Theta}{2}\cos\frac{3\Theta}{2}\right)\right] + \sigma_{ox} \\
\sigma_y &= \frac{1}{2\pi r}\left[K_I\cos\frac{\Theta}{2}\left(1+\sin\frac{\Theta}{2}\sin\frac{3\Theta}{2}\right) + K_{II}\sin\frac{\Theta}{2}\cos\frac{\Theta}{2}\cos\frac{3\Theta}{2}\right] \qquad (1) \\
\tau_{xy} &= \frac{1}{2\pi r}\left[K_I\sin\frac{\Theta}{2}\cos\frac{\Theta}{2}\cos\frac{3\Theta}{2} + K_{II}\cos\frac{\Theta}{2}\left(1-\sin\frac{\Theta}{2}\sin\frac{2\Theta}{2}\right)\right],
\end{aligned}$$

from which:

$$\begin{aligned}
(\sigma_1 - \sigma_2)^2 &= \tfrac{1}{2\pi r}\left[(K_I\sin\Theta + 2K_{II}\cos\Theta)^2 + (K_{II}\sin\Theta)^2\right] - \\
&\quad 2\tfrac{\sigma_{ox}}{\sqrt{2\pi r}}\sin\tfrac{\Theta}{2}\left[K_I\sin\Theta(1+2\cos\Theta) + K_{II}(1+2\cos^2\Theta+\cos\Theta)\right] \\
&\quad +\sigma_{ox}^2
\end{aligned} \qquad (2)$$

By inserting the values $k_\sigma \cdot m_i = \sigma_1 - \sigma_2$ into (1) we obtain the isochromatic curves in polar coordinates (r, Θ). For each isochromatic loop the position of maximum

angle Θ_m corresponds to the maximum radius of the r_m. This principle can also be used in the mixed mode analysis [7] by employing information from two loops in the near field of the crack, if the far field stress component – $\sigma_{ox}(\Theta) = \text{const}$. Differentiating eqn (2) with respect to Θ, setting $\Theta = \Theta_m$ and $r = r_m$ and using $\partial\tau_m/\partial\Theta_m = 0$ gives:

$$g(K_I, K_{II}, \sigma_{ox}) = \frac{1}{2\pi r}\left[K_I^2 \sin 2\Theta + 4K_I K_{II}\cos 2\Theta - 3K_{II}^2 \sin 2\Theta\right]$$
$$-2\frac{\sigma_{ox}}{\sqrt{2\pi r r}} \sin\frac{\Theta}{2}\left\{\left[K_I(\cos\Theta + 2\cos 2\Theta) - K_{II}(2\sin 2\Theta + \sin\Theta)\right]\right.$$
$$\left.+\frac{1}{2}\cos\frac{\Theta}{2}\left[K_i(\sin\Theta + \sin 2\Theta) + K_{II}(2 + \cos 2\Theta + \cos\Theta)\right]\right\}$$

$$f(K_I, K_{II}, \sigma_{ox}) = (\sigma_1 - \sigma_2)^2 - (k_\sigma \cdot m)^2 = 0$$

and

$$g(K_I, K_{II}, \sigma_{ox}) = \frac{\partial[(\sigma_1 - \sigma_2)^2]}{\partial\Theta_m} = 0 \tag{3}$$

(a)

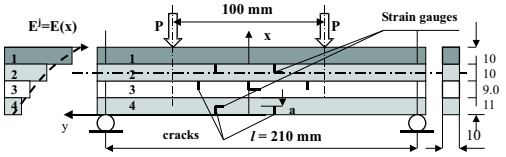

(b)

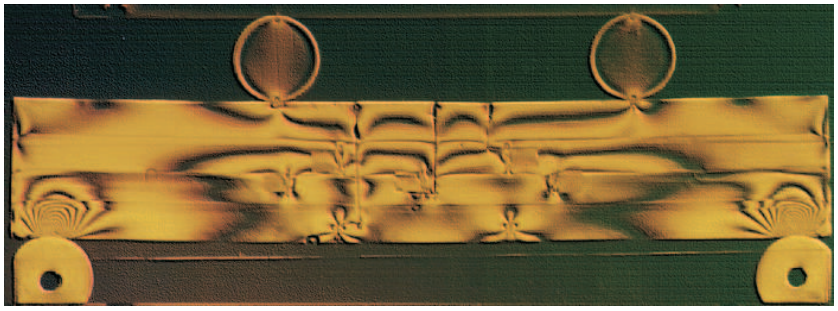

(c)

Figure 1 (a) Four-layer beam with cracks. Photoelastic model under four point bending, the isochromatic patterns ($\sigma_1 - \sigma_2$) distribution, (b) initial loading (P=20.0 N), (c) P=50.0 N - tension of layers 2, 3 and 4.

Substituting the radii r_m and the angles Θ_m from these two loops into a pair of equations of the form given in eqn (3) gives two independent relations dependent

on the parameters K_I, K_{II} and σ_{ox}. The third equation is obtained by using eqn (2). The three equations obtained in this way have the form

$$\begin{aligned} g_i(K_I, K_{II}, \sigma_{ox}) &= 0 \\ g_j(K_I, K_{II}, \sigma_{ox}) &= 0 \\ f_k(K_I, K_{II}, \sigma_{ox}) &= 0 \end{aligned} \tag{4}$$

In order to determine K_I, K_{II} and σ_{ox} it is sufficient to select two arbitrary points r_i, Θ_i and apply the Newton-Raphson method to the solution of three simultaneous non-linear equations (4). The values K_C according to mixed mode of the fracture were obtained from

$$K_C = \sqrt{K_I^2 + K_{II}^2} \tag{5}$$

Example of the numerical results obtained from (4): $m = 12.5$, $r_1 = 0.6$ mm, $\Theta_1 = 1.484$, $r_2 = 10.45$ mm, $\Theta_2 = 1.416$, $K_I^{(4)} = 0.14$ MPa$\sqrt{m}$, $K_{II}^{(4)} = 1.05$ MPa$\sqrt{m}$, $\sigma_{ox} = 0.039$ MPa, $K_C^{(4)} = 1.05$ MPa$\sqrt{m}$.

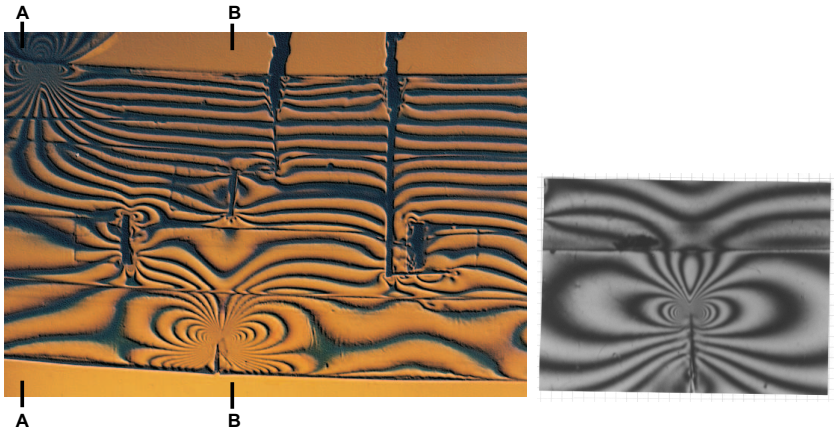

Figure 2 The isochromatic patterns $(\sigma_1 - \sigma_2)$ distribution according to the propagation of the crack obtained experimentally

By inserting the values r_i, Θ_i in three selected arbitrary points into (2) we obtain three non-linear equations $(i = 1, 2, 3)$

$$f_i(K_I, K_{II}, \sigma_{ox}) = 0 \tag{6}$$

and apply the Newton-Raphson method to the solution we have K_I, $K_{II}$and σ_{ox}. Example of the numerical results (shown in Fig. 3) obtained from (6) for: $m_1 = 12.5$, $r_1 = 0.72$ mm, $\Theta_1 = 1.484$, $m_2 = 8.0$, $r_2 = 1.15$ mm, $\Theta_2 = 1.37$, $m_3 = 5.5$ mm, $r_3 = 1.85$, $\Theta_3 = 1.315$, $K_I^{(4)} = 0.702$ MPa$\sqrt{m}$, $K_{II}^{(4)} = 1.043$ MPa$\sqrt{m}$, $\sigma_{ox} = 0.152$ MPa, $K_C^{(4)} = 1.257$ MPa$\sqrt{m}$.

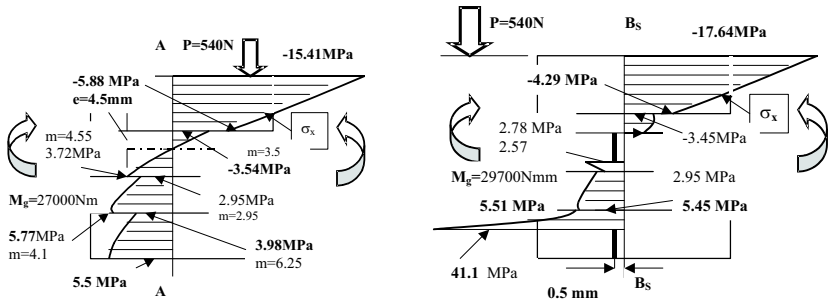

Figure 3 Distribution of stresses σ_x in cross-sections A–A and B–B 0.5mm with respect to crack obtained experimentally

4. Numerical Determination Of Stress Distribution

The distribution of stresses and displacements has been calculated using the finite element method (FEM) [12]. Finite element calculations were performed in order to verify the experimentally observed the isochromatic distribution observe during cracks propagation. The geometry and materials of models were chosen to correspond to the actual specimens used in the experiments. The numerical calculations were carried out using the finite element program ANSYS 6.1 and by applying the substructure technique. For comparison the numerical (from FEM) and experimental sochromatic fringes $(\sigma_1 - \sigma_2)$, distribution was shown in Fig. 3. A finite element mesh of the model (used for numerical simulation) are presented in Fig. 5 and the stresses σ_x are shown in Figs. 6 and 7.

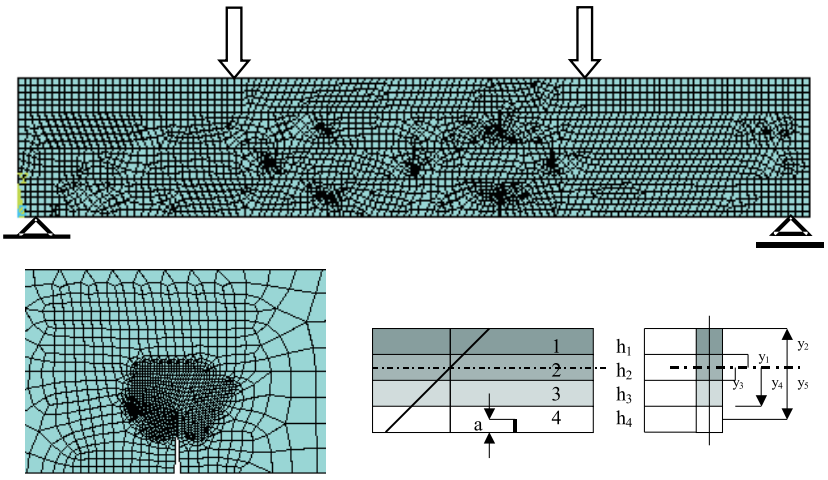

Figure 4 A finite element mesh of the model (for numerical simulation)

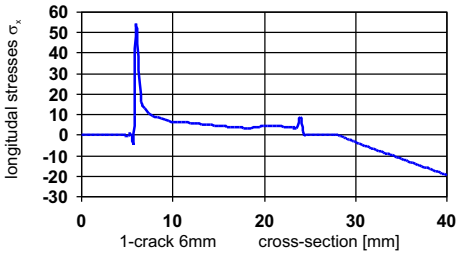

Figure 5 Numerical determination of stress distribution (ANSYS 5.4). Distribution of the stresses σ_x along the crack

The strain energy release rate G_C equal in this case to the Rice J-integral:

$$J = \int_s (\tfrac{1}{2}\sigma_{ij}\varepsilon_{ij}dx_2 - T_i^n \frac{\partial u_i}{\partial x_1} ds)] \tag{7}$$

or from numerical calculation using the finite element method:

$$\begin{aligned} J \quad = \quad & \sum_j \left\{ \frac{1}{2} \left[\frac{1}{E_i} \left(\sigma_{yi}^2 - \sigma_{xi}^2 \right) + \frac{\tau_{xyi}^2}{2G} \right] \cdot n_{1i} - \right. \\ & \left. \left[\frac{\tau_{xyi}}{E_i} \left(\sigma_{xi} - \nu\sigma_{yi} \right) \cdot n_{2i} + \left(\tau_{xyi} n_{1i} + \sigma_{yi} n_{2i} \right) \frac{\Delta\nu_i}{\Delta x_i} \right] \right\} \cdot \Delta S_i \end{aligned} \tag{8}$$

The values K_C according to the fracture in the 4-layer were determined from

$$K_C^{(i)} = \sqrt{E_i \cdot G_C} \tag{9}$$

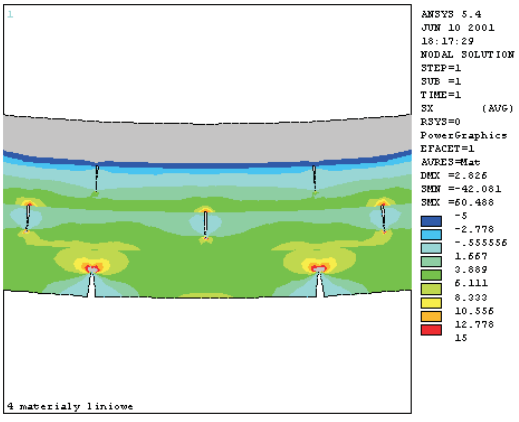

Figure 6 Numerical determination of stress distribution (ANSYS 5.4). Distribution of the stresses σ_x (cracks length a=6.0 mm)

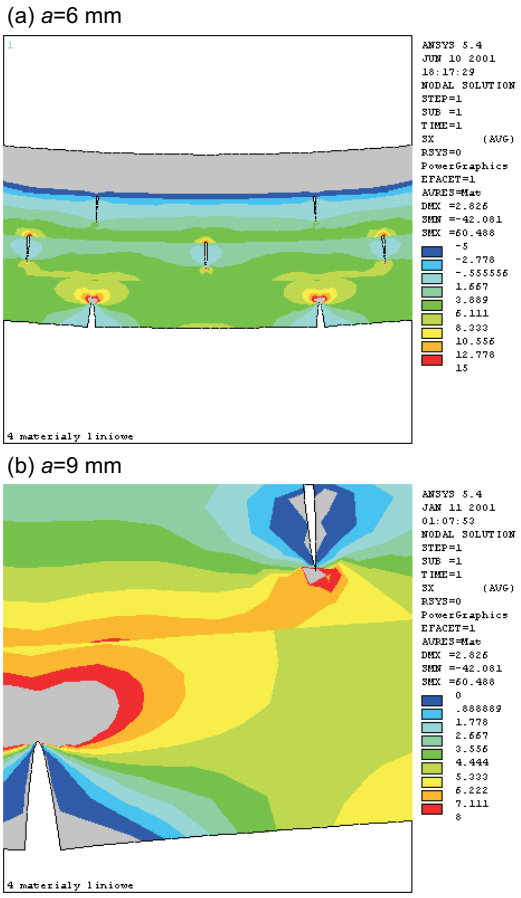

Figure 7 Numerical results: (ANSYS 5.4). Distribution of the stresses σ_x, cracks length (a) $a = 6.0$ mm and (b) $a = 9.0$ mm, thickness of layers $h = 10$ mm

Table 2 Experimental and numerical results. Critical values $K_{IC}^{(1)}$ according to the propagation of the crack and $K_{IC}^{(2)}$

Crack length a [mm]	Critical force P_{cr} [N]	Experimental results [MPa$\sqrt{m}$]				Numerical results [MPa$\sqrt{m}$]	
a	P_{cr}	$K_I^{(4)}$	$K_{II}^{(4)}$	$K_C^{(4)}$	σ_{OX}	$G_C^{(4)}$	$K_C^{(4)}n$
6.0	265.0	1.177	0.8793	**1.419**	2.58	3.08	**1.45**
9.0	205.0	0.702	1.043	**1.257**	0.152	2.39	**1.28**
9.8	185.0	0.14	1.05	**1.05**	0.039	1.97	**1.16**

5. Conclusions

Photoelasticity was shown to be promising in stress analysis of beams with various number and orientation of cracks. It is possible to fabricate a model using various photoelastic materials to model multi layered structure. Finite element calculations (FEM) were performed in order to verify the experimentally observed branching phenomenon and the isochromatic distribution observed during cracks propagation. The agreement between the finite element method predicted isochromatics-fringe patterns distribution and those determined photoelastically was found to be within $3 \div 5$ percent.

References

[1] **Cherepanov, GP**: *Mechanics of Brittle Fracture*, (1979), Mc Graw-Hill, New York.

[2] **Cook, TS** and **Erdogan, F**: Stresses in bonded materials with a crack perpendicular to the interface, *Int. Journ. of Eng. Science*, (1972), **10**, 677-697.

[3] **Frocht, MM**: *Photoelasticity*, (1960), John Wiley, New York.

[4] **Gupta, AG**: Layered composite with a broken laminate, *International Journal of Solids and Structures*, **36**, (1973), 1845-1864.

[5] **Hilton, PD** and **Sin GC**: A laminate composite with a crack normal to interfaces, *International Journal of Solids and Structures*, **7**, (1971), 913.

[6] **Neimitz, A**: *Mechanics of fracture*, (1998), PWN, Warsaw, (in Polish).

[7] **Sanford, RJ** and **Dally, J**: A General Method For Determining Mixed-Mode Stress Intensity Factors From Isochromatic Fringe Patterns, *Eng. Fract. Mech.*, (1979), **2**, 621-633.

[8] **Stupnicki, J**: Trends of experimental mechanics, *Journ. of Theoterical and Applied Mechanics*, (1965), **2**, 34, 207-233.

[9] **Stupnicki, J**, **Olzak, M**, **Wójcik, R**: Numerical analysis of surface crack propagtion in rail-wheel contact zone, *Rail Quality and Maintenance for Modern Railway operation*, (1991), Kluwer Academic, The Netherlands, 385-395.

[10] **Szczepiński, W**: A photoelastic method for determining stresses by means isochromes only, *Archives of Applied Mechanics*, (1961), **5**, 13.

[11] ANSYS User's Guide, 5.4, 5.6, Ansys, Inc., (1999), Huston, USA.

[12] **Zienkiewicz, OC**: *The Finite Element Method in Engineering Science*, (1971), Mc Graw-Hill, London, New York.